Supporting Information

High fluorescence LaOBr/ Coumarin Organic-inorganic composite nanomaterials for ultra-sensitive Fe^{3+} sensing, fluorescence imaging and water-based ink anti-counterfeiting applications

Liheng Sun[a], Jingshi Liu[a], Shihan Xu[b], Biao Dong[a]*, Jiekai Lv[a], Songtao Hu[a], Bingshuai Zhou[a], Bo Shen[a], Yuqi Wang[a], Lin Xu[a], Wen Xu[a], Xue Bai[a], Hongwei Song[a]*

[a]*State Key Laboratory on Integrated Optoelectronics, College of Electronic Science and Engineering, Jilin University, 2699 Qianjin Street, Changchun, 130012, P. R. China.*

[b]*Department of Bioengineering, University of Washington, Seattle, United States.*

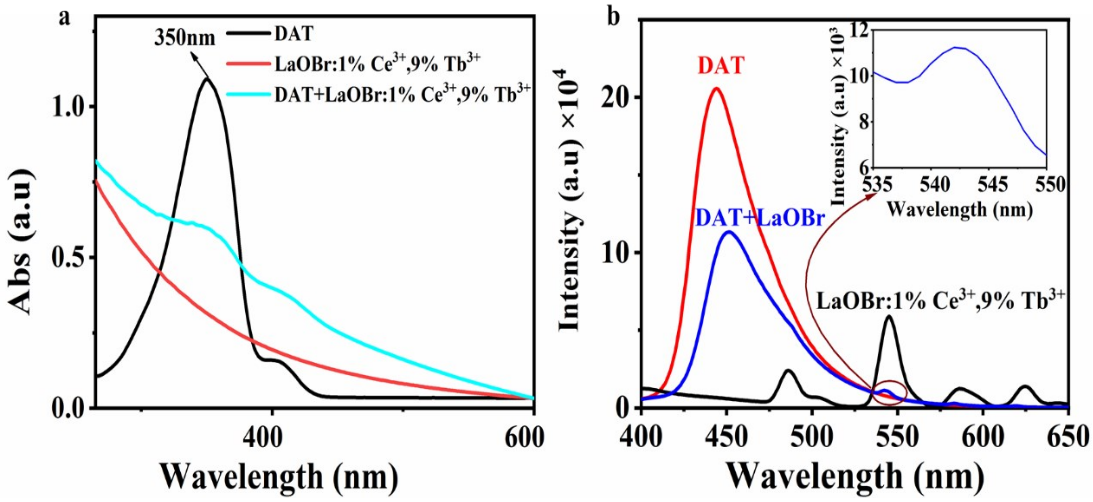

Fig. S1, a Absorption spectra of DAT, LaOBr:1% Ce^{3+},9% Tb^{3+}, and LaOBr/DAT composites; b Emission spectra of DAT, LaOBr and LaOBr/DAT composites.

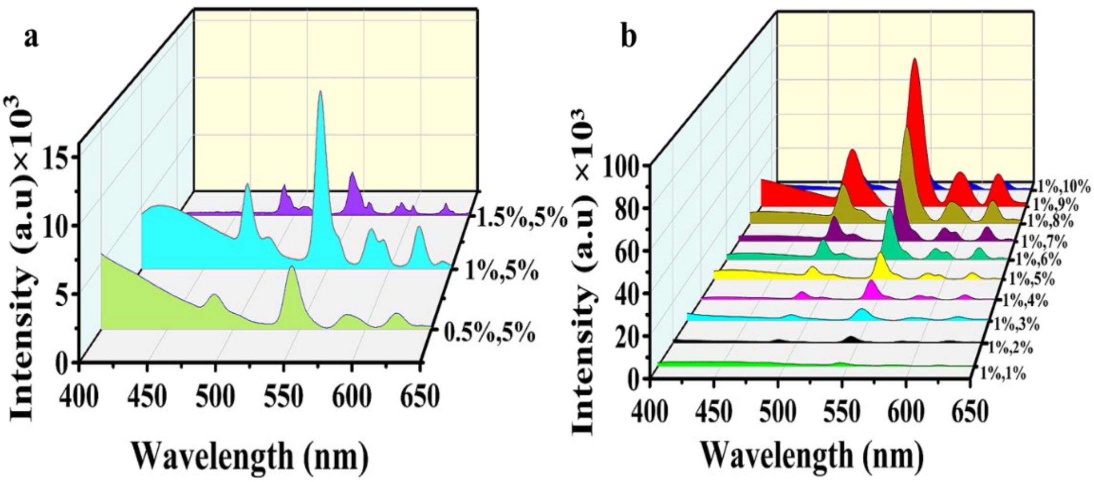

Fig. S2, a Emission spectra of LaOBr : x% Ce^{3+}, 5% Tb^{3+}, b emission spectra of LaOBr : 1% Ce^{3+}, y% Tb^{3+}.

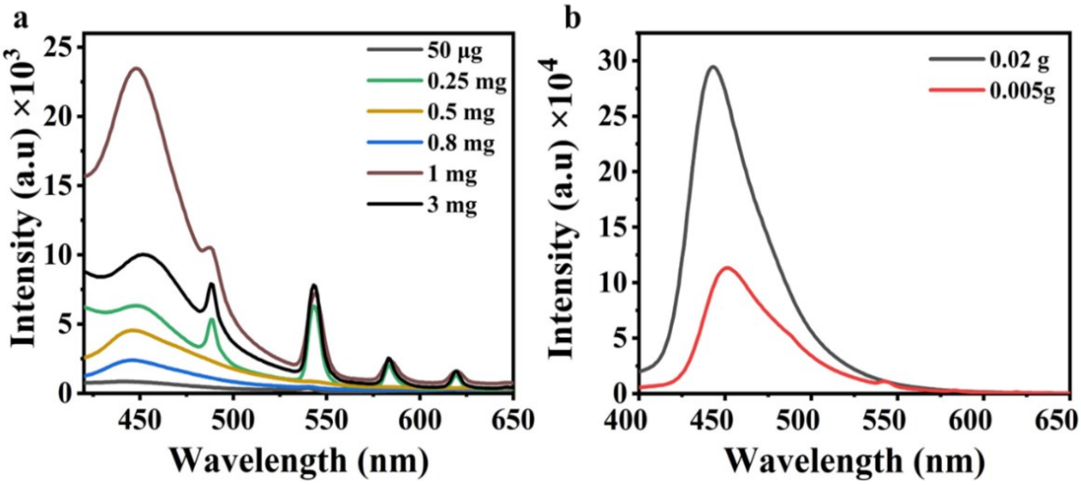

Fig. S3, a, b Emission spectra of composites synthesized by different amounts of DAT.

We got a series of composites with different fluorescence intensity by changing the amount of DAT that was substituted by LaOBr. We found that the ratio fluorescence was related to the substitution amount of DAT.

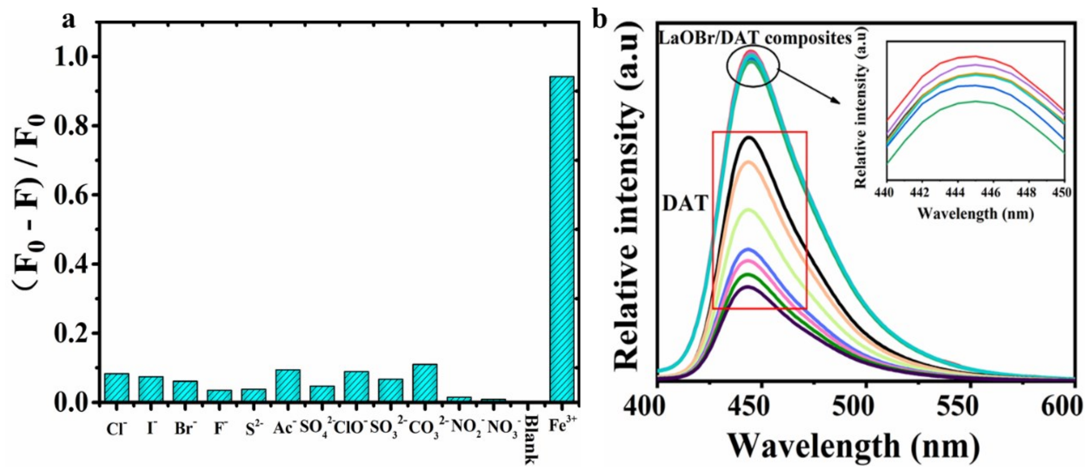

Fig. S4, a The response of iron ions to other anions; b The evolution of the corresponding emission spectra of the stability determination of DAT and LaOBr/DAT composites in Fig. 3(b).

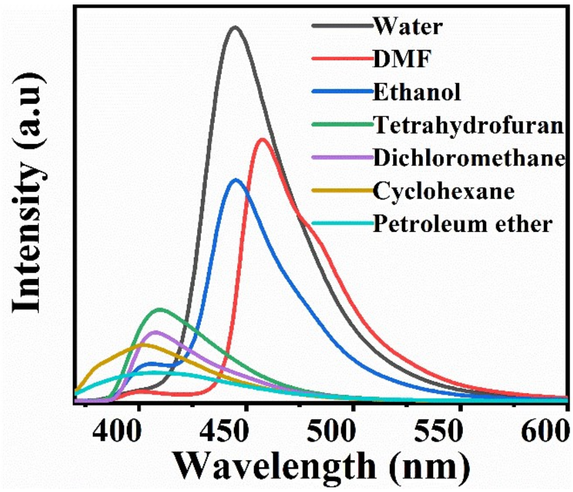

Fig. S5 Emission spectra of DAT in different solvents.

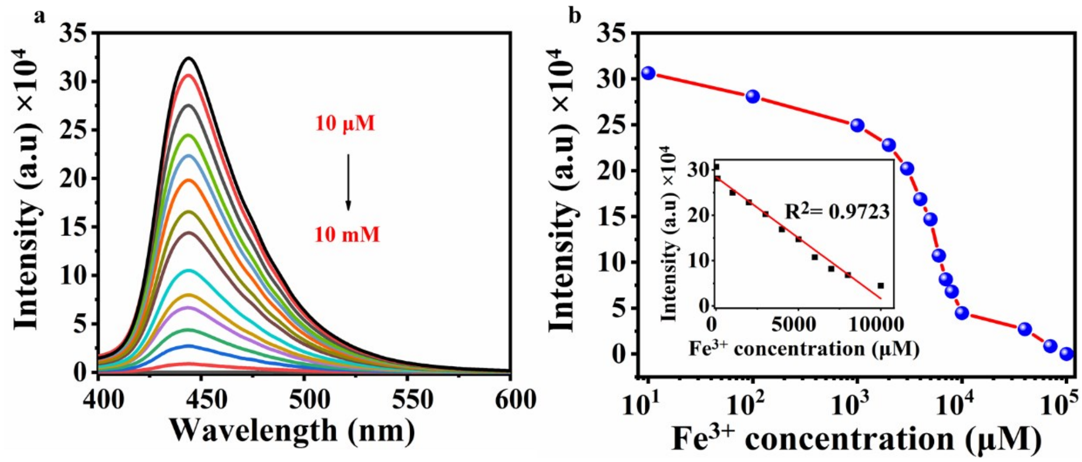

Fig. S6 a Evolution of the spectra of DAT molecules with different iron ion concentration of 10 μM to 10 mM in water; (b) The corresponding linear relationship between fluorescence intensity and Fe^{3+} ions.

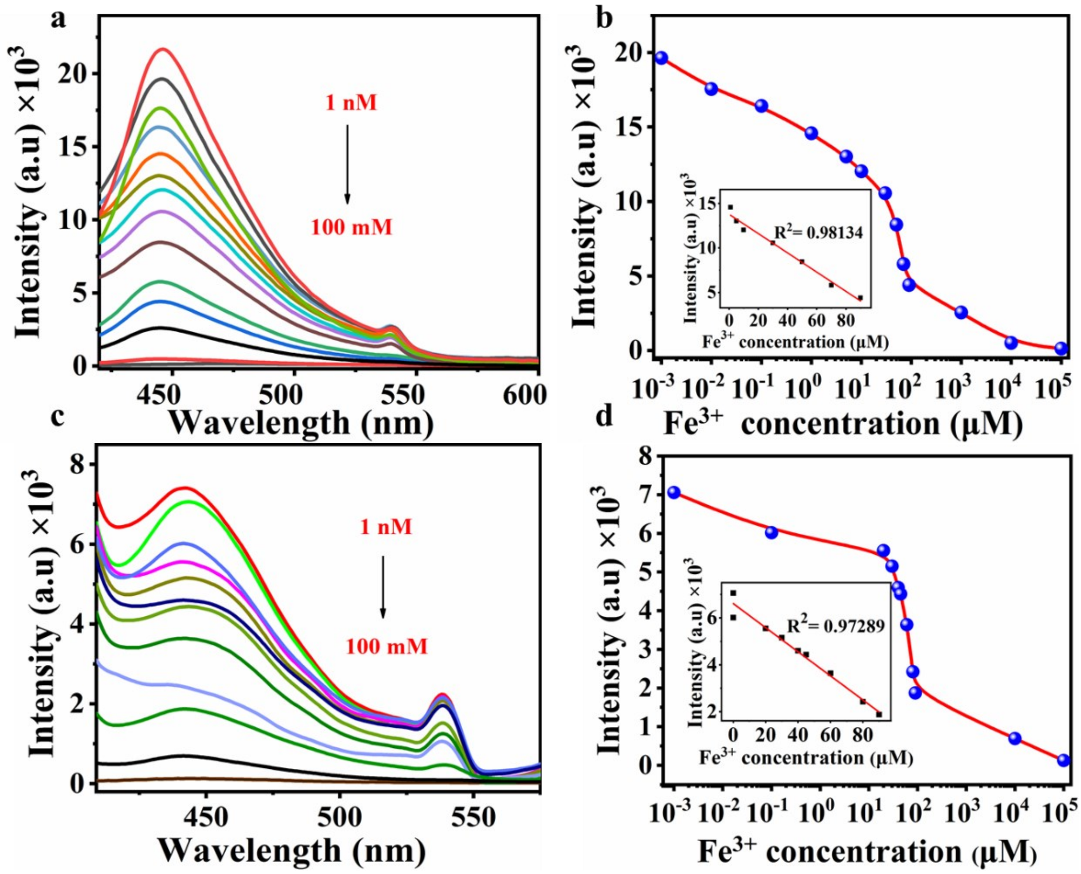

Fig. S7, a, c Evolution of the spectra of LaOBr/DAT composite probes with different iron ion concentration of 1 nM to 100 mM in water and ethanol/water (1:1); (b), (d) The corresponding linear relationship between fluorescence intensity and Fe^{3+} ions.

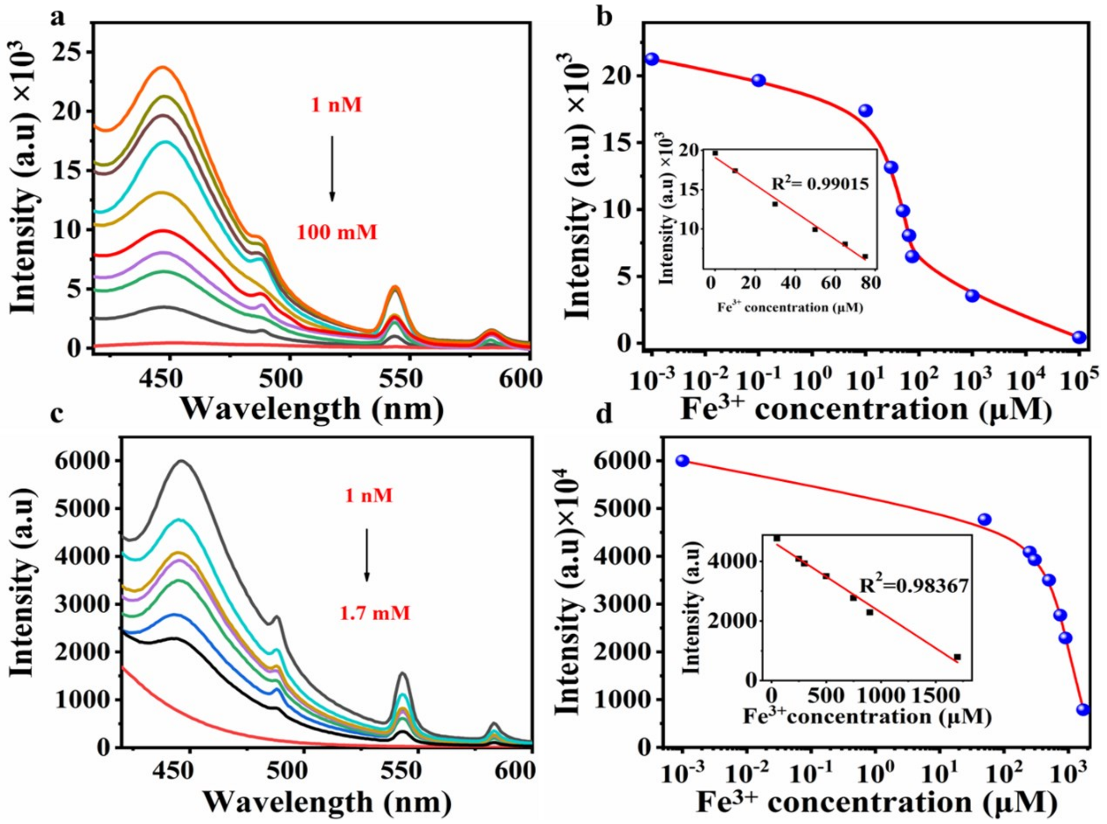

Fig. S8. Evolution of the spectra of LaOBr/DAT composite probes with Fe^{3+} concentration in (a) ethanol (1 nM to 100 mM), as well as in (c) cyclohexane (1 nM to 1.7 mM); (b), (d) The corresponding linear relationship between fluorescence intensity and Fe^{3+} ions, respectively.

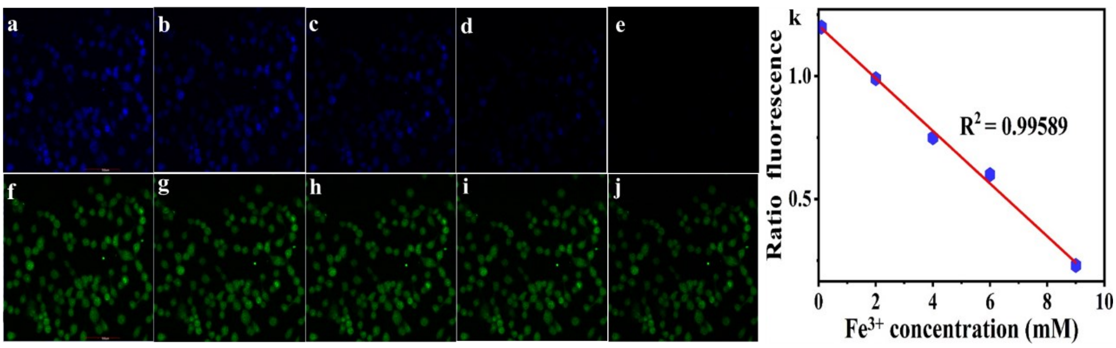

Fig. S9 (a-j) MCF-7 cell imaging and iron ion sensing utilizing the dual-mode luminescence properties of LaOBr/DAT composites and the multi-channel function of confocal microscope. Blue light channel (a-e) shows the weakening images with increasing Fe^{3+} concentration from 100 μM to 10 mM, while green channel (f-j) for LaOBr: 1% Ce^{3+}, 9% Tb^{3+} fluorescence imaging keep stable as the variation of the Fe^{3+} concentration (λ_{ex}=405 nm); (k) Linearity based on the fluorescence gray values of the two imaging channels for the cellular level Fe^{3+} detection from 100 μM to 10 mM.

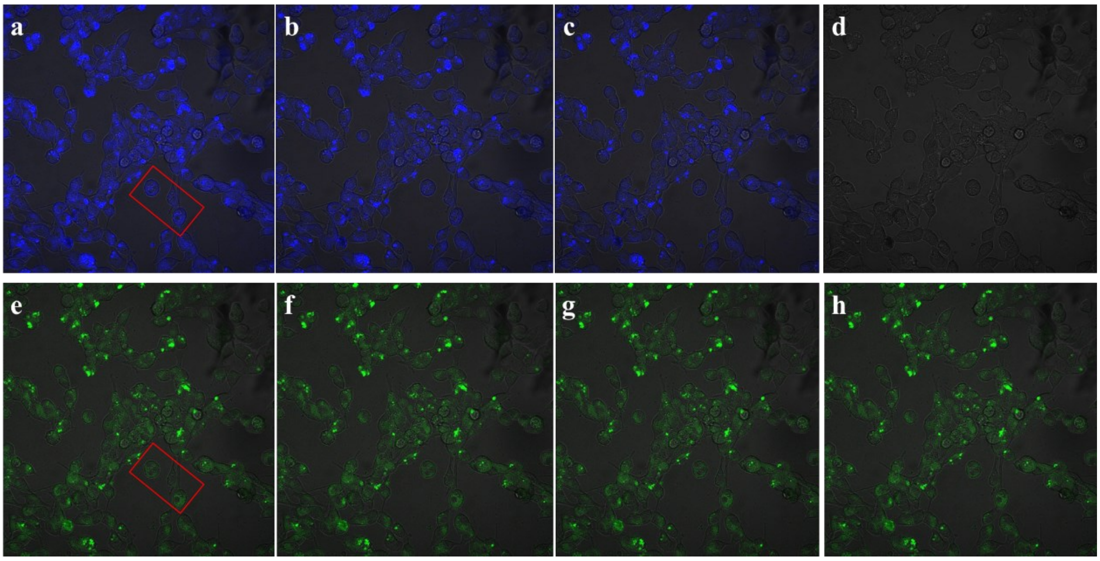

Fig. S10 (a-h) fluorescent images on MCF-7 cells (cells are magnified for 20 times) and iron ion sensing utilizing the dual-mode luminescence properties of LaOBr/DAT composites under two channels of a confocal microscope. The Blue channel (a-d) shows the weakening images as Fe^{3+} concentration increased from 100 μM to 10 mM, while the green channel (e-h) for LaOBr:1% Ce^{3+},9% Tb^{3+} shows fluorescent images keeping stable as Fe^{3+} concentration increased (λ_{ex}=405 nm).

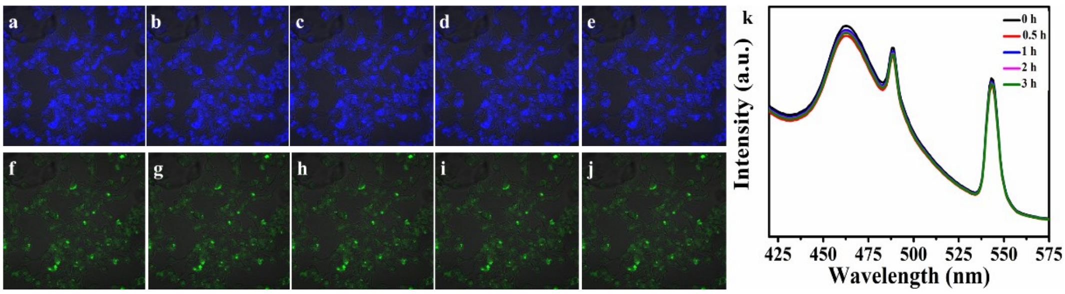

Fig. S11 (a-j) MCF-7 cell imaging at different time intervals under continuous illumination (λ_{ex} = 405 nm) utilizing the dual-mode luminescence properties of LaOBr/DAT composites under two channels of a confocal microscope; Blue light channel (a-e) shows the emission of DAT (458 nm), and green light channel (f-j) shows the emission of LaOBr (540 nm). k Corresponding emission spectrogram were recorded with confocal microscopy.